An experimental proposal to observe non-abelian statistics of Majorana-Shockley fermions in an optical lattice

Dong-Ling Deng,[1,2] Sheng-Tao Wang,[1,2] Kai Sun,[1] and Lu-Ming Duan[1,2]

[1] *Department of Physics, University of Michigan, Ann Arbor, Michigan 48109, USA*
[2] *Center for Quantum Information, IIIS, Tsinghua University, Beijing 100084, PR China*

We propose an experimental scheme to observe non-abelian statistics with cold atoms in a two dimensional optical lattice. We show that the Majorana-Schockley modes associated with line defects obey non-abelian statistics and can be created, braided, and fused, all through adiabatic shift of the local chemical potentials. The detection of the topological qubit is transformed to local measurement of the atom number on a single lattice site. We demonstrate the robustness of the braiding operation by incorporating noise and experiential imperfections in numerical simulations, and show that the requirement fits well with the current experimental technology.

arXiv:1408.5653v1 [quant-ph] 25 Aug 2014

Besides the conventional bosons and fermions, in synthetic two-dimensional (2D) materials there exist more exotic quasi-particles with non-abelian statistics, meaning that the state of the system will be transformed by non-commutable unitary operators when we adiabatically braid the particles one around the other [1]. Search for such non-abelian particles is one of the hottest topics in physics [1–5]. Observation of the non-abelian statistics is of both fundamental interest and practical importance, in particular for topological quantum computation [2, 6] Despite the recent great progress [4, 5, 7–10], it remains technically elusive to braid the quasi-particles in materials to verify their conjectured non-abelian statistics [1].

Laser controlled cold atoms provide a powerful experimental platform to realize exotic states of matter [11–13]. Several proposals have been made to observe non-abelian statistics based on control of vortex states in a $p+ip$ superfluid [14–16]. A vortex in a $p+ip$ superfluid of odd vorticity traps a zero energy mode corresponding to a Majorana fermion, which is its own antiparticle and described by a real fermion operator [3]. The Majorana fermions in different vortices are found to obey non-abelian statistics [17–19]. An intriguing proposal has been made to braid the vortex Majorana fermions in cold atomic gas by a focused laser beam [15, 16]. An experimental implementation of this proposal, however, is still challenging for several reasons: first, besides the Majorana mode a vortex traps a number of other states which have a small gap to the zero-energy mode [15]. This small gap sets a tough requirement for the relevant energy and time scales. Second, moving of the vortex by a focused laser beam may change its trapped modes, and a quantitative understanding of this process is still lacking. Finally, a natural way to realize the $p+ip$ superfluid is based on the p-wave Feshbach resonance [20], but the latter is difficult to stabilize in free space [21, 22]. Very recently, another nice idea has been suggested to braid Majorana modes associated with dislocations in an optical lattice [23]. Insertion of dislocations requires change of structure of the optical lattice, which is experimentally challenging and yet to be demonstrated.

In this paper, we propose an experimental scheme to observe non-abelian statistics with cold atoms in an optical lattice in a vortex-free configuration. A p-wave superfluid based on the Feshbach resonance could be stabilized in an optical lattice due to the quantum Zeno effect [22, 24]. The recent remarkable experimental advance has allowed single-site addressing in a 2D optical lattice [25–29]. By this ability, we can create a line defect in a 2D lattice simply by shifting the chemical potential along the line. Different from the dislocations, this line defect requires no change of structure of the optical lattice and is ready to be implemented in current experiments [25–29]. It was found recently that a pair of zero-energy modes emerge at the edges of this line defect [30] by the Shockley mechanism [31]. The exchange statistics of these modes, however, remains unresolved [30]. Motivated by recent works on braiding of nanowires [32], here we show through exact numerical simulation that the Majorana-Shockley modes associated with these line defects in a 2D superfluid obey non-abelian statistics and their braiding can be achieved by tuning of only the local chemical potential. This tuning is significantly simpler compared with the braiding of nanowires [32] or dislocations [23], which requires site-by-site tuning of the pairing interaction and the tunneling rates [32, 33]. We demonstrate robustness of the braiding operation under influence of practical noise and propose a scheme to measure the topological qubits using local measurement of the atom number. The proposed scheme fits well with the state-of-the-art of the experimental technology in a 2D optical lattice [25–29].

We consider cold atoms in a 2D optical lattice, which are prepared into the $p+ip$ superfluid phase. This superfluid phase can be achieved, for instance, through the p-wave Feshbach resonance [20], which leads to the $p+ip$ superfluid phase under a wide range of experimental parameters [20]. The instability associated with the p-wave Feshbach resonance in free space [21] could be overcome in an optical lattice through the quantum Zeno effect [22]. Alternatively, an effective $p+ip$ superfluid phase for cold atoms can also be achieved by a combination

of the s-wave Feshbach resonance and the light induced spin-orbital coupling [16, 34, 35].

In the momentum $\mathbf{k}$ space, the Bogoliubov-de Gennes (BdG) Hamiltonian describing the $p+ip$ superfluid phase on a square optical lattice has the form $H = \sum_{\mathbf{k}} \psi_{\mathbf{k}}^{\dagger} \mathcal{H}(\mathbf{k}) \psi_{\mathbf{k}}$, with $\psi_{\mathbf{k}}^{\dagger} = (c_{\mathbf{k}}^{\dagger}, c_{-\mathbf{k}})$ and

$$\mathcal{H}(\mathbf{k}) = d_x(\mathbf{k})\sigma^x + d_y(\mathbf{k})\sigma^y + d_z(\mathbf{k})\sigma^z, \qquad (1)$$

where $d_x(\mathbf{k}) = \Delta \sin k_x a$, $d_y(\mathbf{k}) = \Delta \sin k_y a$, $d_z(\mathbf{k}) = \mu - J(\cos k_x a + \cos k_y a)$, $\sigma^{x,y,z}$ denote the Pauli matrices, a is the lattice constant, μ is the chemical potential, J is the neighboring hopping rate, and Δ is the pairing interaction strength. The topological property of this Hamiltonian is characterized by the first Chern number $C_1 = -\frac{1}{2\pi}\int_{\mathrm{BZ}} dk_x dk_y F_{xy}(\mathbf{k})$ with the Berry curvature $F_{xy}(\mathbf{k}) = \partial_{k_x} A_y(\mathbf{k}) - \partial_{k_y} A_x(\mathbf{k})$ and the Berry connection $A_\nu(\mathbf{k}) = \langle u_-(\mathbf{k}) | i\partial_{k_\nu} | u_-(\mathbf{k})\rangle$ $(\nu = x, y)$, where $|u_-(\mathbf{k})\rangle$ denotes the lower band Bloch eigenstate of $\mathcal{H}(\mathbf{k})$ and the integration in C_1 is over the first Brillouin zone (BZ). The phase of the Hamiltonian H is topologically nontrivial with $C_1 = \mathrm{sign}(\mu)$ in the parameter regime $0 < |\mu| < 2J$ (taking Δ as the energy unit) and topologically trivial with $C_1 = 0$ when $|\mu| > 2J$. A topological phase transition occurs at $|\mu| = 2J$.

With single-site addressing, the potential shift of each lattice site can be individually adjusted in experiments [25–29]. We create a line defect in a 2D optical lattice by tuning the chemical potential μ_d along a chain of atoms to make it different from that of the background lattice (denoted by μ_0) so that they reside in topologically distinct phases (illustrated in Fig. 1a). For a certain range of μ_d that depends on μ_0, a pair of zero energy Majorana-Shockley fermion (MSF) modes appear at the two edges of the line defect [30]. We choose μ_0 in the topologically trivial phase with $\mu_0 > 2J$ so that there are no other zero-energy modes on the boundary of the finite 2D lattice.

Under a typical size of the 2D optical lattice with a line defect, we solve exactly the eigenmodes of the Hamiltonian (1) under the open boundary condition, and the eigen-spectrum is shown in Fig. 1b (see Methods). Clearly, there are a pair of zero-energy MSF modes that are separated from other defect modes and bulk states by a minimum gap about J. The MSFs are described by anti-commuting real fermion operators γ_j with $\gamma_j = \gamma_j^{\dagger}$ and $\gamma_j\gamma_k + \gamma_k\gamma_j = 2\delta_{jk}$. A pair of MSF modes γ_1 and γ_2 together represent a conventional fermion mode $c_m = (\gamma_1 + i\gamma_2)/2$, with the eigenstates of $c_m^{\dagger}c_m = i\gamma_1\gamma_2 + 1$ encoding a topological qubit. The eigen-functions of the MSF modes γ_1 and γ_2 are shown in Fig. 1c, which are well localized at the edges of the line defect.

To examine the exchange statistic of the MSF modes, we adiabatically deform the line defect with steps shown in Fig. 2(a-f). Each step is achieved through site-by-site tuning of the chemical potential from μ_d to μ_0 (to shorten the line defect) or from μ_0 to μ_d (to extend the line defect). We simulate the time evolution of the MSF modes in the Heisenberg picture under adiabatic evolution of the Hamiltonian. The Hamiltonian remains gapped at any time as shown in Fig. 2g, which protects the MSF modes from mixing of the other modes. The evolution of the MSF modes γ_1 and γ_2 and their correlation are shown in Fig. 2h. After the whole evolution with time T, apparently we have $\gamma_1(T) = \gamma_2(0)$ and $\gamma_2(T) = -\gamma_1(0)$. The correlation $\langle \gamma_1(T)\gamma_2(T)\rangle = -\langle \gamma_2(0)\gamma_1(0)\rangle = \langle \gamma_1(0)\gamma_2(0)\rangle$.

This transformation of the MSF modes occurs in a similar way when we adiabatically braid the edges associated with different line defects. In Fig. 3a, we illustrate the adiabatic braiding of two edge modes γ_2 and γ_3 of different line defects along a T-junction path. This braiding involves joining and cutting of two line defects and we need to choose parameters appropriately to avoid appearance of accidental near-zero-energy modes. In general, the four zero-energy MSF modes are still well protected by a significant energy gap. Their evolution and the associated correlations are shown in Fig. 3b. The results indicate that $\gamma_2(T) = \gamma_3(0)$ and $\gamma_3(T) = -\gamma_2(0)$ for the

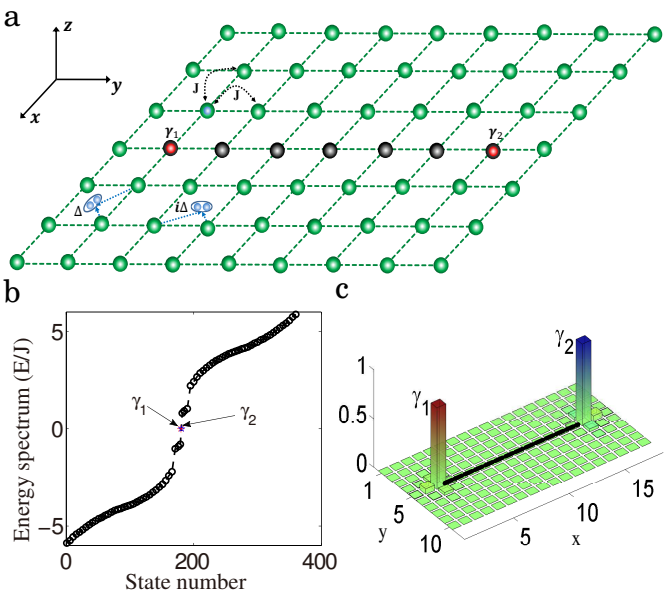

FIG. 1. **Creation and manipulation of the MSFs in an optical lattice.** (**a**) Cold fermionic atoms are loaded into a 2D optical lattice. J and Δ denotes the nearest neighbor hopping rate and pairing strength. A line defect with different local chemical potential binds two zero-energy MSFs γ_1 and γ_2 (red circles) at its edges. (**b**) Energy spectrum of the Hamiltonian H on a square lattice of size $18a \times 10a$ with open boundaries. The length of the line defect is $14a$. The zero-energy MSFs have tiny energy splitting due to the small size of the line defect, which is numerically found to be $< 10^{-10}J$ for our parameters. (**c**) The amplitude of the mode function for γ_1 and γ_2. The black line indicates the line defect with chemical potential μ_d. The parameters are chosen as $\Delta = J$, $\mu_0 = 10J$, and $\mu_d = 0.1J$.

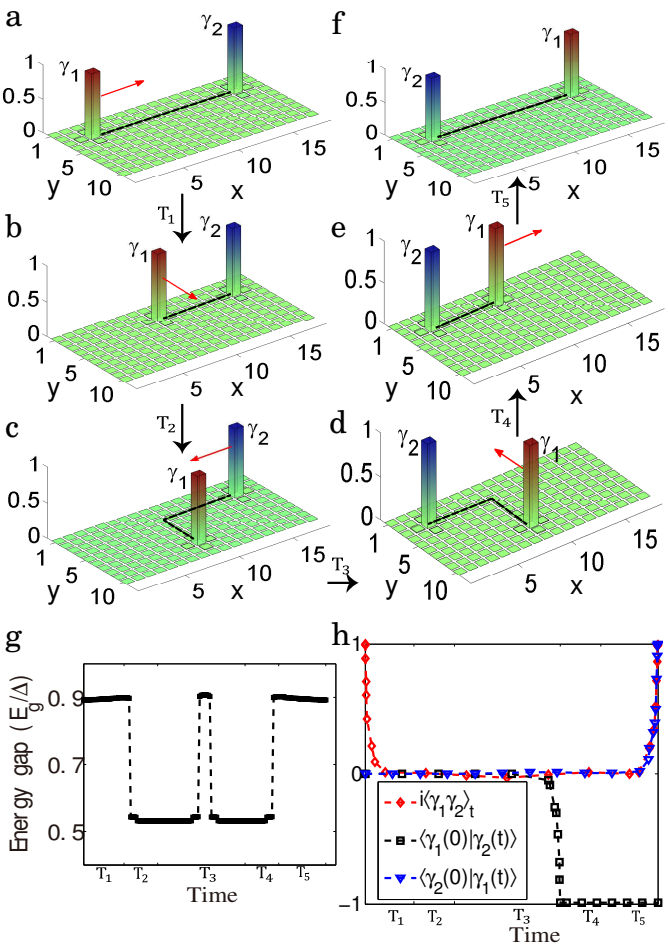

FIG. 2. **Braiding of two MSFs bound to the same line defect.** (**a**) The black line indicates the line defect with chemical potential μ_d. Sequentially tuning the local chemical potentials at one end from μ_d to μ_0 shortens the line defect and transports γ_1 along the x direction. The red arrow shows the moving direction of the MSF. Similar operations along a T-junction path realize adiabatic exchange of γ_1 and γ_2, with steps illustrated in (**a**)-(**f**). (**g**) The evolution of the energy gap E_g throughout the braiding process. The system is always gapped with the minimum gap $E_g > 0.5J$. (**h**) Time evolution of the MSF modes γ_1, γ_2 and their correlations. All the parameters are the same as in Fig. 1.

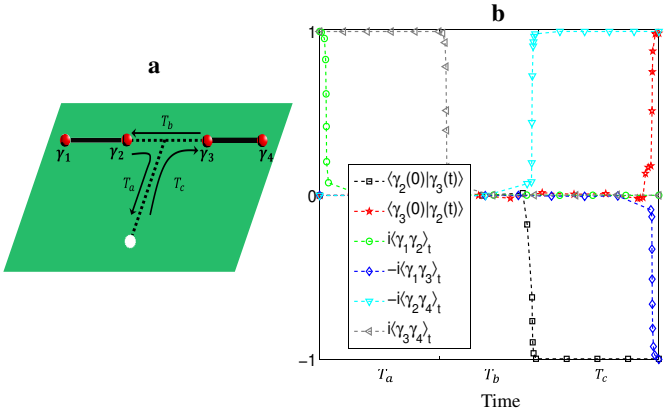

FIG. 3. **Braiding of two MSFs bound to different line defects.** (**a**) Illustration of braiding two MSFs from different line defects along the T-junction path. (**b**) Time evolution of the MSF modes $\gamma_1, \gamma_2, \gamma_3, \gamma_4$ and their correlations. The MSFs γ_2 and γ_3 are braided. The parameters are taken as: the lattice size $12a \times 28a$, two horizontal line defects each of length $8a$ and distance $9a$, $\Delta = 0.91J$, $\mu_0 = 10\Delta$ and $\mu_d = 0.1\Delta$.

two braided modes. The other modes remain unchanged with $\gamma_1(T) = \gamma_1(0)$ and $\gamma_4(T) = \gamma_4(0)$.

The above transformation rule generalizes straightforwardly to the case of $2N$ MSF modes. The rule is exactly the same as the case of Majorana fermions bound to vortices. For $2N$ modes γ_j $(j = 1, 2, \cdots, 2N)$, when we braid γ_j and γ_{j+1}, the transformation is described by a unitary operator $U_j = e^{\pi\gamma_{j+1}\gamma_j/4}$ which transforms $\gamma_j \to \gamma_{j+1}, \gamma_{j+1} \to -\gamma_j$. As U_j and U_{j+1} do not commute, the exchange statistics of the MSF modes are non-abelian and belongs to the so-called Ising anyon class according to classification of non-abelian anyons [36].

The unitary operation U_j from topological braiding of the MSF modes are robust to noise and experimental imperfections. To test that, we consider several sources of noise typical for atomic experiments: First, with imperfect single-site addressing, when we tune the chemical potential of one site, we may change the potentials of the neighboring sites as well, modeled by a spreading ratio of $1 - \alpha$. Second, there is a global weak harmonic trap for cold atom experiments, with an additional trapping potential $V_{\text{trap}} = \frac{V_T}{2(L_x^2+L_y^2)} \sum_{\mathbf{r}} d_{\mathbf{r}}^2 c_{\mathbf{r}}^\dagger c_{\mathbf{r}}$, where L_x (L_y) is the lattice dimension along the x (y) direction, and $d_{\mathbf{r}}$ is the distance from the trap center. Typically, V_T ranges from $0.1J$ to J. Finally, there is unavoidable small disorder potential in experiments which adds random fluctuation to the chemical potential with magnitude denote by λ_R. We recalculate the evolution of the MSF modes and their correlation, incorporating contribution of all these sources of noise. The results are shown in Fig. 4, which are almost indistinguishable from the corresponding results shown in Fig. 2h under the ideal case. This demonstrates robustness of the braiding operations of the MSFs.

To verify the non-abelian braiding operations, we need to detect the topological qubit encoded by two nonlocal MSF modes γ_1 and γ_2. For the 1D nanowire, the parity of the total particle number is a conserved property, which is different for the two eigenstates of $i\gamma_1\gamma_2$ and thus can be used to detect the topological qubit [32, 33]. For our case, the line defect interacts with the background lattice with tunneling and pairing terms which in general do not conserve the parity of the total atom number along the line, therefore the parity detection does not work. We propose a different method to detect the topological qubit. The line defect is adiabatically shortened until it

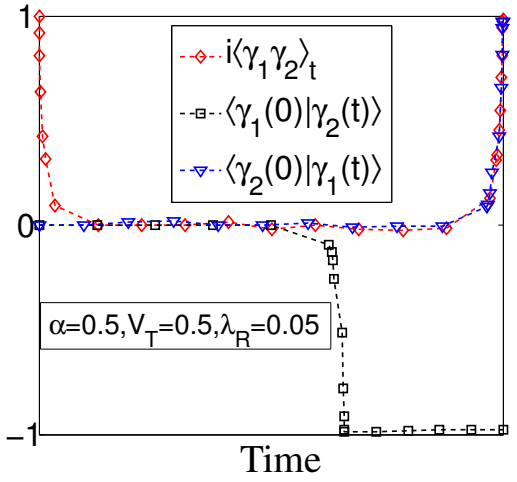

FIG. 4. **Robustness to experimental noise and imperfections.** The lattice size is $20a \times 12a$ and other parameters are the same as in Fig. 1. α, V_T, λ_R denote the parameters characterizing respectively the laser beam crosstalk, the strength of the global harmonic trap, and the magnitude of random fluctuation of the chemical potential (see the main text).

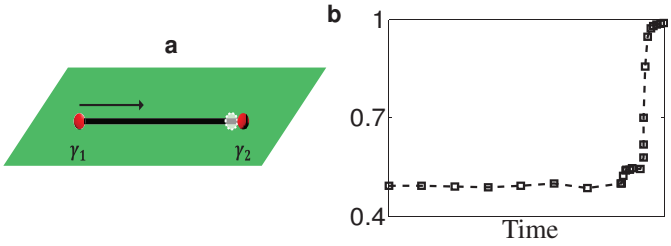

FIG. 5. **Detection of the topological qubit.** (**a**) Two MSFs γ_1 and γ_2 are fused through adiabatic shortening of the line defect to a single lattice site $\mathbf{r}_0$. (**b**) Transformation of the MSF modes γ_1 and γ_2 under adiabatic merging. For simplicity, we plot evolution of the magnitude of the mode overlap between $c_{\mathbf{r}_0}$ and $[\gamma_1(t) + i\gamma_2(t)]/2$. At the end of merging, γ_1 and γ_2 are mapped dominantly to the local modes $c^\dagger_{\mathbf{r}_0} + c_{\mathbf{r}_0}$ and $i(c^\dagger_{\mathbf{r}_0} - c_{\mathbf{r}_0})$, respectively, which enables detection of the initial nonlocal topological qubit by a simple measurement of the atom number $c^\dagger_{\mathbf{r}_0} c_{\mathbf{r}_0}$ on a single lattice site after the adiabatic merging. All the parameters are the same as in Fig. 1.

finally reduces to a single lattice site $\mathbf{r}_0$ (illustrated in Fig. 5a) and we examine evolution of the MSF modes γ_1 and γ_2 during this process. As shown in Fig. 5b, with a high fidelity (about 99%), the mode γ_1 (γ_2) is mapped to $\gamma_{\mathbf{r}_0,A} = c^\dagger_{\mathbf{r}_0} + c_{\mathbf{r}_0}$ ($\gamma_{\mathbf{r}_0,B} = i(c^\dagger_{\mathbf{r}_0} - c_{\mathbf{r}_0})$), respectively. By a measurement of the local atom number $c^\dagger_{\mathbf{r}_0} c_{\mathbf{r}_0}$ after the adiabatic merging, we thus measure the topological operator $i\gamma_1\gamma_2$ with a high fidelity (about 98%). This local measurement is actually more robust compared with the nonlocal parity detection. Note that the detection fidelity of the topological qubit in principle can be improved to an arbitrary accuracy by using the quantum non-demolition (QND) technique: to measure the topological qubit $i\gamma_1\gamma_2$, we create an ancillary topological qubit (with MSF modes γ_3 and γ_4), perform an effective Controlled-NOT gate between the topological qubits $i\gamma_1\gamma_2$ and $i\gamma_3\gamma_4$ through the noise-resilient braiding operations [37]., and then measure the ancilla $i\gamma_3\gamma_4$ by the above method. As the qubit $i\gamma_1\gamma_2$ is not destroyed by the measurement, it can be repeatedly measured through this QND technique and the detection error is exponentially suppressed with increase of the detection rounds.

In summary, we have proposed a complete scheme to observe non-abelian statistics of the MSFs associated with line defects in a 2D optical lattice. The MSFs are created, braided, and fused all through adiabatic tuning of the chemical potential for certain lattice sites. The detection of the topological qubit is transformed to local measurement of the atom number on a single lattice site. The required technology well fits with the current status of the optical lattice experiments [25–29]. Through numerical simulation, we have demonstrated robustness of the non-abelian braiding operations under typical experimental configuration with imperfections. The scheme provides a viable approach for observation of the exotic non-abelian braiding statistics, which is a goal of intense interest and a critical step for realization of robust topological quantum information processing [2, 6, 37].

Appendix

Time evolution. We first Fourier transform the Hamiltonian (1) into real space, with the modes in real space denoted by $c_{\mathbf{r}}$. A line defect has chemical potential μ_d instead of μ_0. We define the Majorana operators at each lattice site with $\gamma_{\mathbf{r},A} = (c^\dagger_{\mathbf{r}} + c_{\mathbf{r}})$ and $\gamma_{\mathbf{r},B} = i(c^\dagger_{\mathbf{r}} - c_{\mathbf{r}})$. In terms of these Majorana operators, the Hamiltonian has the following form:

$$H = \frac{i}{2} \sum_{\mathbf{p},\mathbf{q}} \mathcal{H}_{\mathbf{pq}} \gamma_{\mathbf{p}} \gamma_{\mathbf{q}}, \tag{2}$$

where $p = (\mathbf{r}, \beta)$ and $q = (\mathbf{r}', \beta')$ ($\beta, \beta' = A, B$) are combined indices and $\mathcal{H}$ is a $2N \times 2N$ real skew-symmetric matrix with N being the number of lattice sites.

By locally and adiabatically tuning μ along a T-junction path, MSFs can be braided. During this process, the Majorana operators evolve according to the following equation in the Heisenberg picture [38]:

$$\gamma_{\mathbf{p}} \to \gamma_{\mathbf{p}}(t) = U \gamma_{\mathbf{p}}(0) U^\dagger = \sum_{\mathbf{q}} \mathcal{O}_{\mathbf{qp}} \gamma_{\mathbf{q}}(0), \tag{3}$$

where $U = \mathcal{T} \exp[i \int_0^t H(\tau) d\tau]$ and $\mathcal{O} = \mathcal{T} \exp[-i \int_0^t \mathcal{H}(\tau) d\tau]$ is an element of the special orthogonal group $\mathcal{O} \in \mathrm{SO}(2N)$; $\mathcal{T}$ is the time-ordering operator.

In our numerical simulation, we first diagonalize $\mathcal{H}$ at time $t = 0$ to obtain the zero-energy eigen modes

$\gamma_i(0) = \sum_{\mathbf{p}} \eta_{i\mathbf{p}} \gamma_{\mathbf{p}}(0)$, where the coefficients $\eta_{i\mathbf{p}}$ represent the mode function and are localized at the ends of the line defects. During the braiding process, the zero-energy eigen modes evolve as $\gamma_i(t) = U\gamma_i(0)U^\dagger = \sum_{\mathbf{p}} \eta_{i\mathbf{p}} \gamma_{\mathbf{p}}(t)$, where $\gamma_{\mathbf{p}}(t)$ are calculated via Eq. (3). Using this method, we obtain the time evolution of the zero-energy MSF modes with the results plotted in the main text.

Majorana correlation functions. To calculate the Majorana correlations, we use the method introduced in Ref. [39]. Let us define the density operator $\rho = N\exp(-\beta H)$ (N is the normalization constant and β is the inverse temperature) and the antisymmetric covariance matrix Γ with elements $\Gamma_{\mathbf{pq}} = \frac{i}{2}\mathrm{Tr}[\rho(\gamma_{\mathbf{p}}\gamma_{\mathbf{q}} - \gamma_{\mathbf{q}}\gamma_{\mathbf{p}})]$. The Hamiltonian H can be brought into block off-diagonal form $OHO^{\mathrm{T}} = \oplus_{j=1}^{N} \begin{pmatrix} 0 & -\epsilon_j \\ \epsilon_j & 0 \end{pmatrix}$ by a special orthogonal matrix $O \in \mathrm{SO}(2N)$, where ϵ_j characterizes the energy eigen-spectrum of the Hamiltonian. This matrix O also reduces Γ to a block off-diagonal form $O\Gamma O^{\mathrm{T}} = \oplus_{j=1}^{N} \begin{pmatrix} 0 & \eta_j \\ -\eta_j & 0 \end{pmatrix}$ with $\eta_j = \tanh(\beta\epsilon_j/2)$. The covariance matrix Γ_{G} corresponding to the ground state of H is obtained by letting the inverse temperature $\beta \to \infty$, i.e., $\eta_j \to \mathrm{sgn}(\epsilon_j)$. After we obtain Γ_{G}, the Majorana correlations can be computed by Wick's theorem via the equation:

$$i\langle\gamma_{\mathbf{p}}\gamma_{\mathbf{q}}\rangle = \mathrm{Pf}(\Gamma_{\mathrm{G}}^{'}), \tag{4}$$

where $\Gamma_{\mathrm{G}}^{'} = \begin{pmatrix} (\Gamma_{\mathrm{G}})_{\mathbf{pp}} & (\Gamma_{\mathrm{G}})_{\mathbf{pq}} \\ (\Gamma_{\mathrm{G}})_{\mathbf{qp}} & (\Gamma_{\mathrm{G}})_{\mathbf{qq}} \end{pmatrix}$ is a 2×2 submatrix of Γ_{G} and $\mathrm{Pf}(\Gamma_{\mathrm{G}}^{'})$ is the Pfaffian of $\Gamma_{\mathrm{G}}^{'}$ with $\mathrm{Pf}(\Gamma_{\mathrm{G}}^{'})^2 = \det(\Gamma_{\mathrm{G}}^{'})$. Once we have obtained $i\langle\gamma_{\mathbf{p}}\gamma_{\mathbf{q}}\rangle$ at time $t = 0$, the time evolution of the MSF mode correlations $i\langle\gamma_i\gamma_j\rangle_t$ can be computed directly using $\gamma_i(t) = \sum_{\mathbf{p}} \eta_{i\mathbf{p}}\gamma_{\mathbf{p}}(t) = \sum_{\mathbf{p},\mathbf{q}} \eta_{i\mathbf{p}}\mathcal{O}_{\mathbf{qp}}\gamma_{\mathbf{q}}(0)$.

Acknowledgement We thank J. Alicea, C. V. Kraus, and Y.-H Chan for discussions. D.L.D., S.T.W., and L.M.D. are supported by the NBRPC (973 Program) 2011CBA00300 (2011CBA00302), the IARPA MUSIQC program, the ARO and the AFOSR MURI program. K.S. is supported in part by NSF PHY-1402971.

Author contributions All the authors contribute substantially to this work.

Competing financial interests The authors declare no competing financial interests.

[1] Stern, A. Non-abelian states of matter. *Nature* **464**, 187-193 (2010).

[2] Nayak, C., Simon, S. H., Stern, A., Freedman, M. & Das Sarma, S. Non-abelian anyons and topological quantum computation. *Rev. Mod. Phys.* **80** 1083-1159 (2008).

[3] Wilczek, F. Majorana returns. *Nat. Phys.* **5**, 614-618 (2009).

[4] Alicea, J. New directions in the pursuit of majorana fermions in solid state systems. *Rep. Prog. Phys.* **75**, 076501 (2012).

[5] Beenakker, C. W. J. Search for majorana fermions in superconductors. *Annu. Rev. Condens. Matter Phys.* **4**, 113-136 (2013).

[6] Kitaev, A. Y. Fault-tolerant quantum computation by anyons. *Ann. Phys.* **303** 2-30 (2003).

[7] Mourik, V. *et. al.* Signatures of majorana fermions in hybrid superconductor-semiconductor nanowire devices. *Science* **336**, 1003-1007 (2012).

[8] Das, A. *et. al.* Zero-bias peaks and splitting in an alinas nanowire topological superconductor as a signature of majorana fermions. *Nat. Phys.* **8**, 887-895 (2012).

[9] Rokhinson, L. P., Liu, X. Y. & Furdyna, J. K. The fractional ac josephson effect in a semiconductor-superconductor nanowire as a signature of majorana particles. *Nat. Phys.* **8** 795-799 (2012).

[10] Veldhorst, M. *et. al.* Josephson supercurrent through a topological insulator surface state. *Nat. Mater.* **11**, 417-421 (2012).

[11] Dalibard, J., Gerbier, F., Juzeliūnas, G. & Öhberg, P. Colloquium: Artificial gauge potentials for neutral atoms. *Rev. Mod. Phys.* **83**, 1523-1543 (2011).

[12] Bloch, I., Dalibard,J. & Nascimbène, S. Quantum simulations with ultracold quantum gases. *Nat. Phys.* **8** 267-276 (2012).

[13] Lewenstein, M., Sanpera, A., & Ahufinger, V. *Ultracold Atoms in Optical Lattices: Simulating quantum many-body systems.* (Oxford University Press, 2012).

[14] Sato, M., Takahashi, Y. & Fujimoto, S. Non-abelian topological order in s-wave superfluids of ultracold fermionic atoms. *Phys. Rev. Lett.* **103**, 020401 (2009).

[15] Tewari, S., Das Sarma, S., Nayak, C., Zhang, C. W. & Zoller, P. Quantum computation using vortices and majorana zero modes of a $p_x + ip_y$ superfluid of fermionic cold atoms. *Phys. Rev. Lett.* **98** 010506 (2007).

[16] Zhu, S. L., Shao, L. B., Wang, Z. D. & Duan, L. M. Probing non-abelian statistics of majorana fermions in ultracold atomic superfluid. *Phys. Rev. Lett.* **106**, 100404 (2011).

[17] Read, N. & Green, D. Paired states of fermions in two dimensions with breaking of parity and time-reversal symmetries and the fractional quantum hall effect. *Phys. Rev. B* **61** 10267 (2000).

[18] Ivanov, D. A. Non-abelian statistics of half-quantum vortices in p-wave superconductors. *Phys. Rev. Lett.* **86**, 268-271 (2001).

[19] Stern, A., von Oppen, F. & Mariani, Eros. Geometric phases and quantum entanglement as building blocks for non-abelian quasiparticle statistics. *Phys. Rev. B* **70** 205338 (2004).

[20] Gurarie, V., Radzihovsky, L., & Andreev, A. V. Quantum phase transitions across a p-wave feshbach resonance. *Phys. Rev. Lett.* **94** 230403 (2005).

[21] Gaebler, J. P., Stewart, J. T., Bohn, J. L. & Jin, D. S. p-wave feshbach molecules. *Phys. Rev. Lett.*, **98** 200403 (2007).

[22] Han, Y. J. *et. al.* Stabilization of the p-wave superfluid state in an optical lattice. *Phys. Rev. Lett.* **103** 070404 (2009).

[23] Bühler, A. *et. al.* Majorana modes and p-wave superfluids for fermionic atoms in optical lattices. *Nat. Commun.* **4**,

4504 (2014).

[24] Syassen, N. *et. al.* Strong dissipation inhibits losses and induces correlations in cold molecular gases. *Science* **320**, 1329-1331 (2008).

[25] Sherson, J. F. *et. al.* Single-atom-resolved fluorescence imaging of an atomic mott insulator. *Nature* **467** 68-72 (2010).

[26] Weitenberg, C. *et. al.* Single-spin addressing in an atomic mott insulator. *Nature* **471**, 319-324 (2011).

[27] Bakr, W. S., Gillen, J. I., Peng, A., Fölling, S. & Greiner, Markus. A quantum gas microscope for detecting single atoms in a hubbard-regime optical lattice. *Nature* **462**, 74-77 (2009).

[28] Bakr, W. S. *et. al.* Probing the superfluid-to-mott insulator transition at the single-atom level. *Science* **329**, 547-550 (2010).

[29] Wurtz, P., Langen, T., Gericke, T., Koglbauer, A. & Ott, H. Experimental demonstration of single-site addressability in a two-dimensional optical lattice. *Phys. Rev. Lett.* **103** 080404 (2009).

[30] Wimmer, M., Akhmerov, A. R., Medvedyeva, M. V., Tworzydło, J. & Beenakker, C. W. J. Majorana bound states without vortices in topological superconductors with electrostatic defects. *Phys. Rev. Lett.* **105**, 046803 (2010).

[31] Shockley, W. On the surface states associated with a periodic potential. *Phys. Rev.* **56** 317-323 (1939).

[32] Alicea, J., Oreg, Y., Refael, G., von Oppen, F. & Fisher, M. P. A. Non-abelian statistics and topological quantum information processing in 1d wire networks. *Nat. Phys.* **7**, 412-417 (2011).

[33] Kraus, C. V., Zoller, P. & Baranov, M. A. Braiding of atomic majorana fermions in wire networks and implementation of the deutsch-jozsa algorithm. *Phys. Rev. Lett.* **111**, 203001 (2013).

[34] Fu, L. & Kane, C. L. Superconducting proximity effect and majorana fermions at the surface of a topological insulator. *Phys. Rev. Lett.* **100**, 096407 (2008).

[35] Sau, J. D., Lutchyn, R. M., Tewari, S. & Sarma, S. D. Generic new platform for topological quantum computation using semiconductor heterostructures. *Phys. Rev. Lett.* **104** 040502 (2010).

[36] Francesco, P. D., Senechal D. & Mathieu, P. Conformal field theory. (Springer, 1997).

[37] Deng, D. L. & Duan, L. M. Fault-tolerant quantum random-number generator certified by majorana fermions. *Phys. Rev. A*, **88**, 012323 (2013).

[38] Kraus, C. V., Wolf, M. M. & Cirac, J. I. Quantum simulations under translational symmetry. *Phys. Rev. A* **75** 022303 (2007).

[39] Kraus, C. V., Wolf, M. M., Cirac, J. I. & Giedke, G. Pairing in fermionic systems: A quantum-information perspective. *Phys. Rev. A* **79**, 012306 (2009).